Effects of the body force on the evacuation dynamics

I.M. Sticco[a], G.A. Frank[b], C.O. Dorso[a,c,*]

[a] *Departamento de Física, Facultad de Ciencias Exactas y Naturales, Universidad de Buenos Aires, Pabellón I, Ciudad Universitaria, 1428 Buenos Aires, Argentina.*
[b] *Unidad de Investigación y Desarrollo de las Ingenierías, Universidad Tecnológica Nacional, Facultad Regional Buenos Aires, Av. Medrano 951, 1179 Buenos Aires, Argentina.*
[c] *Instituto de Física de Buenos Aires, Pabellón I, Ciudad Universitaria, 1428 Buenos Aires, Argentina.*

Abstract

Keywords:
Pedestrian Dynamics, Social Force Model, Body Force
PACS: 45.70.Vn, 89.65.Lm

1. Introduction

The Social Force Model (SFM) addresses two physical forces as *essential*: the "body force" and the "sliding friction". Both are inspired by granular interactions and were claimed to be necessary for attaining the particular effects in panicking crowds [1]. The "sliding friction" actually proved to be an essential feature of the "faster-is-slower" effect, although the role of the "body force" appears, at a first instance, not so clear [2, 3, 4].

The existence of a "body force" in the context of highly dense crowds (say, 5 to 10 people/m^2) is a commonsense matter [5, 6]. Researchers, however, question the numerical setting for this force in the SFM context [7]. As a matter of fact, the usual setting by Helbing prevents the overlapping among pedestrians, but it is known to accomplish artificially high force levels [1, 7, 8, 9]. The force estimates from the SFM appear to be remarkably higher with respect to the reported real life data (say, an order of magnitude). The

*codorso@df.uba.ar

crowd motion simulations, however, present quite realistic results [7, 8, 10]. The point seems to be that the SFM focuses on the "incoordination phenomenon" due to clogging, missing the "individualistic" perspective of single pedestrians or very small groups [1, 5, 11].

Many researchers realized that modifying the SFM may (partially) surpass the misleading parameter setting. It was proposed that the pedestrians' psychological force (say, the "social force") should be suppressed in the context of highly dense crowds [12, 13, 14, 15], or smoothly quenched according to the crowd density [16]. The authors in Refs. [17, 18] further proposed a rigid body model in order to completely avoid the overlapping phenomenon. This perspective dismisses any connection to a "sliding friction". Conversely, other authors tried to limit the pedestrians acceleration by introducing "static friction" between the pedestrians and the floor [19]. This kind of friction, however, reduces the effective willings of the pedestrians.

A meaningful (individualistic) numerical setting appears not available yet (to our knowledge). The reason is that different numerical settings can lead to the same crowd dynamics. Actually, only a small set of dimensionless "numbers" control the crowd dynamics [20]. These are similar to those encountered in other active matter systems (Péclet number, etc.) [21]. We may hypothesize that while the dimensionless "numbers" provide some kind of control on the "incoordination phenomenon" in crowds, only a few numerical settings can attain an "individualistic" meaning.

The numerical setting for the "faster is slower" effect presented by Helbing and co-workers is somewhat cumbersome Ref. [1, 10, 20]. Although a single parameter (say, the desired velocity v_d) is numerically varied to explain the phenomenon, the researcher looses sight of the dimensionless "numbers" that truly control the crowd dynamics. The setting in Ref. [1] also misses the "faster is faster" effect reported to occur at very high pedestrian densities [10, 22]. Alternatively, the empirical fundamental diagram raises as a point of reference for the SFM control parameters [23, 10].

The fundamental diagram exhibits the flux behavior for either low dense crowds (with seldom contacts between pedestrians) and highly dense crowds (dominated by body forces and sliding friction). The latter usually experiences a flux slowing down, but other behaviors are also possible [23, 24].

In light of our previous hypothesis, we may suspect that the modeling of the "flux slowing down" within the context of the SFM will require the proper setting of the (dimensionless) controlling parameters. We examined this working hypothesis in Ref. [20], but limiting the parameter exploration to the sliding friction, disregarding the body force.

We now widen the investigation on the parameter settings to include the one associated to the body force. We will focus on the complex interplay between the body force and the sliding friction among pedestrians. Recall that the interplay dynamics is not directly controlled by the numerical setting, but through dimensionless "numbers", where the model parameters appear mixed between each other. Thus, this step up offers a challenge to the "individualistic" meaning of the parameter's setting.

The investigation is organized as follows. We first recall the available experimental values on the body force and the sliding friction (see Section 2). Secondly, we introduce the reduced-in-units SFM and the three dimensionless numbers that control the crowd dynamics (see Section 3). We present our numerical simulations in Section 4. For the sake of clarity, this Section is separated into two major parts: the bottleneck scenario and the corridor scenario in Sections 4.1 and 4.2, respectively. Section 5 opens a detailed discussion raising from of the results in Section 4. The last Section closes the investigation with our main conclusions.

2. Experimental background

The complex behavior of pedestrians feature either his (her) feelings and the environmental conditions. The former is expressed, for example, by his (her) moving "attitude" (say, self-assuredness). The latter brings out the observed separation between pedestrians. Also, the "contacts" between individuals address some kind of "unwanted" slowing down. All these observed patterns are commonly quantified in the literature into a set of characteristic parameters. The experimental meaning of these parameters is as follows.

(i) The walking attitude of a pedestrian may appear somewhat "assertive" if he (she) reacts actively to unexpected behaviors [7, 25]. The smaller the reaction time, the more assertive or aggresive observed posture. The associated parameter to this behavior is the relaxation or characteristic time τ [26, 1].

τ[s]	m[kg]	v_d[m/s]	B[m]	k[kg/s^2]	Refs.
0.61	—	1.24	$0.36 + 1.06\,v$	—	[30]
0.50*	80*	1.34	0.50	—	[28, 7]
—	67.5	1.39	—	$96.1 + 12694.1\,x$	[16]
—	67.0	1.39	—	$97.0 + 29378.9\,x$	[16]

Table 1: The experimental data for the pedestrian parameters, as explained in Section 2. The magnitude v means de pedestrian velocity (m/s). The magnitude x means the compression length (m). The upper row for Ref. [16] corresponds data acquired in winter and the lower row to datas acquiquired in summer. The asterisk (*) corresponds to reasonable estimates from the authors.

(ii) Despite the reactive attitude τ, the pedestrian addresses a "free" (undisturbed) walking speed v_0. This speed expresses his (her) motivation or intention to reach a certain destination (as comfortable as possible). Observations commonly associate 0.6 m/s, 1 m/s or 1.5 m/s to relaxed, normal or nervous walking speeds, respectively [25, 1, 27].

(iii) The walking speed of pedestrians appears to be lower in a crowded walkway with respect to their usually expected "free" walking speeds [28, 7]. Pedestrians tend to reduce their speed within crowded environments because they perceive not enough space for taking a step [26]. This (perceived) step distance is therefore an influential parameter on the pedestrians behavior. It is known as the characteristic length B.

(iv) Physical interactions occur in very crowded environments. The "body force" and "sliding friction" can be introduced straight forward. This will be done in Section 3. But it is worth noting that both are associated to the moving difficulties (say, slowing down and obstructions) observed in contacting pedestrians.

Table 1 shows a few empirical figures for the most common parameters. More data is available throughout the literature (see, for example, Refs. [29, 30, 31, 32, 33, 34, 27]). We intentionally omitted data that assumes a specific mathematical model. The exhibited values should also be considered as a general purpose approach, since no distinction has been made on age, gender or cultural habits.

A first examination of the figures in Table 1 shows that the choise $\tau \simeq 0.6$ s seems to be a reasonable estimation for the relaxation time, although this

may vary with respect to gender or culture [35]. Additionally, we confirm that normal pedestrians attain desired velocities around 1.3 m/s.

The reports from Refs. [30, 28] do not include any values for the compressibility k since these experiments were carried out under low density conditions. Notice that the minimum (perceived) step distance is 0.36 m [30], but the pedestrians seem to require larger distances when they walk faster. The commonly accepted value $B \simeq 0.5\,\mathrm{m}$ is somewhat valid for walking speeds under 0.5 m/s [30]. Higher walking speeds (say, 1 m/s) will require a step distance of 1.3 m for the pedestrians to feel that there is enough space to move along.

The reported data from Ref. [16] correspond to the crowded environment of the Beijing subway. This environment was not suitable for providing information on the step distance B, but estimates for the desired speed and the body compresibility could be achieved. The reported magnitude k assesses either the clothes and the body compressibility. The final value, though, is linearly related to the compression x.

We measured the maximum attainable forces at the subway in Buenos Aires, Argentina. Our preliminary results show that pedestrians feel "uncomfortable" whenever a body force ranging from 5 to 20 N is applied for at least ten minutes. Short lasting forces (say, less than 4 minutes) may also be perceived as "uncomfortable" for values ranging from 10 to 30 N. We also recorded body forces up to 60 N during very short "hits". The comparison with the fittings provided by Ref. [16] shows that these magnitudes accomplish densities around 5 people/m^2.

The maximum (realistic) compressions may be computed from the relation $F = k(x)\,x$ and the compressibility $k(x)$ reported in Table 1. An "uncomfortable" body force of 30 N can address compressions in the range of $0.030 - 0.055\,\mathrm{m}$. Also, a "hitting" force of 60 N can address compressions between 0.045 and 0.065 m. Thus, according to Table 1, we may expect experimental values for $k(x)$ up to $1000\,\mathrm{kg/s}^2$ (for $F = 30\,\mathrm{N}$), or, up to $1400\,\mathrm{kg/s}^2$ (for $F = 60\,\mathrm{N}$).

Besides, no realiable values for the sliding friction κ appears to be available in the literature (to our knowledge). We may pressume, however, that

the sliding friction approaches a fraction of the body force. We will come back to this issue in Section 3.

3. Theoretical background

3.1. The Social Force Model

The Social Force Model (SFM) provides the necessary framework for simulating the collective dynamics of self-driven particles (*i.e.* pedestrians). The pedestrians are considered to follow an equation of motion involving either "socio-psychological" forces and physical forces (say, granular forces). The equation of motion for any pedestrian i (of mass m_i) reads

$$m_i \frac{d\mathbf{v}_i}{dt} = \mathbf{f}_d^{(i)} + \sum_{j=1}^{N} \mathbf{f}_s^{(ij)} + \sum_{j=1}^{N} \mathbf{f}_g^{(ij)} \tag{1}$$

where the subscript j corrresponds to any neighboring pedestrian or the walls. The three forces $\mathbf{f}_d$, $\mathbf{f}_s$ and $\mathbf{f}_g$ are different in nature. The desire force $\mathbf{f}_d$ represents the acceleration (or deceleration) of the pedestrian due to his (her) own willings. The social force $\mathbf{f}_s$, intead, describes the tendency of the pedestrians to stay away from each other. The granular force $\mathbf{f}_g$ stands for either the sliding friction and the compression between pedestrians.

Notice that these forces are supposed to influence the behavior of the pedestrians in a similar fashion as mentioned in Section 2. Thus, the set of (empirical) parameters described in Section 2 is expected to be also present in the SFM. These will appear in connection to the forces, although their meaning may be somewhat different.

The pedestrians' own willing is modeled by the desire force $\mathbf{f}_d$. This force stands for the acceleration (deceleration) required to reach a certain position at the desired walking speed v_d. This involves, however, a personal attitude that makes him (her) appear more or less "assertive". As mentioned in Section 2, the reaction time τ attains for this attitude. Thus, the desire force is modeled as follows

$$\mathbf{f}_d^{(i)} = m \, \frac{v_d^{(i)} \, \hat{\mathbf{e}}_d^{(i)}(t) - \mathbf{v}^{(i)}(t)}{\tau} \tag{2}$$

where $\hat{\mathbf{e}}(t)$ represents the unit vector pointing to the target position. $\mathbf{v}(t)$ stands for the pedestrian velocity at time t.

The tendency of any individual to preserve his (her) "private sphere" is accomplished by the social force $\mathbf{f}_s$. This force is expected to prevent the pedestrians from getting too close to each other (or to the walls) in a crowded environment. If he (she) perceives that there is not enough space to move, he (she) will decelerate or even move back. The model for this kind of "socio-psychological" behavior is as follows

$$\mathbf{f}_s^{(i)} = A\, e^{(R_{ij}-r_{ij})/B}\, \hat{\mathbf{n}}_{ij} \tag{3}$$

where r_{ij} means the distance between the center of mass of the pedestrians i and j, and $R_{ij} = R_i + R_j$ is the sum of the pedestrians radius. The unit vector $\hat{\mathbf{n}}_{ij}$ points from pedestrian j to pedestrian i, meaning a repulsive interaction.

The net distance $|R_{ij} - r_{ij}|$ scales to the parameter B in the expression (3). This parameter plays the role of a fall-off length within the model, and thus, it may be somewhat connected to the (perceived) step distance mentioned in Section 2. The parameter A, however, does not provide any direct link to other parameters mentioned there.

The granular force (say, the sliding friction plus the body force) attain to the moving difficulties encountered in very crowded environments. The expression for the granular force is has been borrowed from other granular matter fields, as follows

$$\mathbf{f}_g^{(ij)} = \kappa\, g(R_{ij} - r_{ij})\, (\Delta\mathbf{v}^{(ij)} \cdot \hat{\mathbf{t}}_{ij})\, \hat{\mathbf{t}}_{ij} + k\, g(R_{ij} - r_{ij})\ \hat{\mathbf{n}}_{ij} \tag{4}$$

where $g(R_{ij} - r_{ij})$ equals $R_{ij} - r_{ij}$ if $R_{ij} > r_{ij}$ and vanished otherwise. $\Delta\mathbf{v}^{(ij)} \cdot \hat{\mathbf{t}}_{ij}$ represents the difference between the tangential velocities of the sliding bodies (or between the individual and the walls).

The sliding friction occurs in the tangential direction while the body force occurs in the normal direction. Both are assumed to be linear with respect to the net distance between contacting pedestrians. The sliding friction is also linearly related to the difference between the (tangential) velocities. The coefficients κ (for the sliding friction) and k (for the body force) are supposed

to be related to the areas of contact and the clothes material, among others.

We stress that the expression (4) assumes fixed values for κ and k. This may not be completely true according to Table 1. The local density (and thus, the pedestrians' compression) may affect the compressibility parameter k by more than an order of magnitude. We will vary k (and κ) in order to explore this phenomenon.

3.2. The parameters setting

The numerical setting of the parameters may affect the dynamics of the pedestrians. Some settings, however, yield similar collective dynamics. In order to investigate these similarities, we introduce unit-less magnitudes and proceed straightforward as indicated in Appendix A. We realize from Appendix A that only three (unit-less) parameters are the true "control" parameters for the collective dynamics. These are $\mathcal{A}$, $\mathcal{K}$, $\mathcal{K}_c$ as defined in Appendix A. Recall that $\mathcal{A}$ and $\mathcal{K}$ are precisely the same as in Ref. [20], but a novel $\mathcal{K}_c$ parameter has been introduced due to the body force.

The logical relations between the unit-less parameters and the "individual" parameters can be studied by means of the Venn diagrams exhibited in Fig. 1. The parameters $\mathcal{A}$, $\mathcal{K}$ and $\mathcal{K}_c$ are represented as intersecting sets, and the "individual" parameters are represented as elements within each set. The shared elements between $\mathcal{A}$, $\mathcal{K}$ and $\mathcal{K}_c$ are placed inside de intersecting regions.

A first inspection of the diagrams in Fig. 1 shows that the relaxation time (per unit mass) τ/m is always a common parameter to all sets, regardless of the body force. This means that the "assertive" attitude of the pedestrian, addressed by the reaction time (see Section 2), applies to all stimuli and the own willings. The role of τ has already been discussed in Refs. [26, 20].

Fig. 1a represents the situation when $\mathcal{K}_c$ is absent. Notice that A/v_d or κB may control the collective dynamic, in spite of the "assertive" attitude. The individual character of v_d or B appears somehow "loosely" in the crowd dynamic. We mean by "loosely" that any numerical setting of these parameters may be counterbalanced by the right setting of A or κ, keeping the

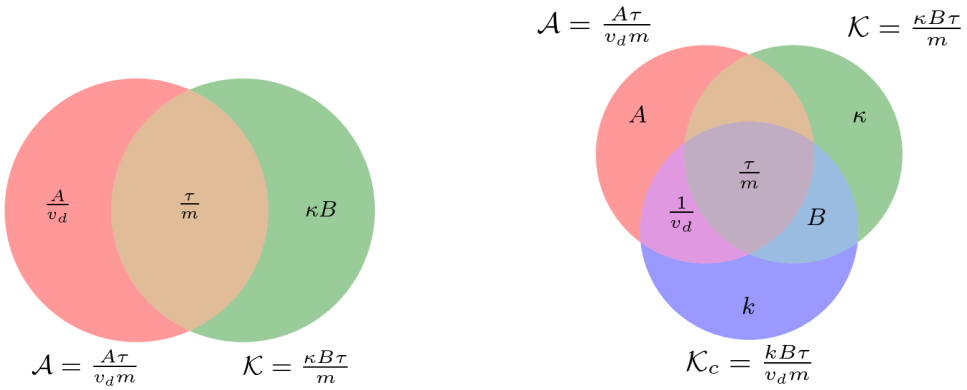

Figure 1: Venn diagrams for the unit-less parameters appearing in the equation of motion (1) (see Appendix Appendix A for details). The sets correspond to $\mathcal{A} = \{\tau/m, 1/v_d, A\}$, $\mathcal{K} = \{\tau/m, B, \kappa\}$ and $\mathcal{K}_c = \{\tau/m, 1/v_d, B, k\}$. (a) The Venn diagram representation if no body force is introduced in the SFM (only sets $\mathcal{A}$ and $\mathcal{K}$, as in Ref. [20]). (b) The Venn diagram representation for the sets $\mathcal{A}$, $\mathcal{K}$ and $\mathcal{K}_c$.

colletive dynamic (qualitatively) unchanged.

Fig. 1b provides a picture of the parameters' relations after introducing $\mathcal{K}_c$. Surprisingly, $\mathcal{K}_c$ appears as a wider set (say, a four elements set) than $\mathcal{A}$ or $\mathcal{K}$ (three elements' sets). It shares the parameter v_d with $\mathcal{A}$ and the parameter B with $\mathcal{K}$. The practical consequence to these (logical) relations is that v_d or B affect simultaneously two "control" parameters of the collective dynamics. Conversely, either v_d and B may counterbalance $\mathcal{K}_c$ in order to keep the colletive dynamic (qualitatively) unchanged.

We confirm from these diagrams that no univocal relations can be established between the individual parameters and the collective dynamics (in a crowded environment). The presence of the body force moves the dynamics to a more complex context. We will investigate this context in Section 4.

4. Results

4.1. Bottleneck

In this section, we present the results corresponding to the bottleneck geometry. We show how the overall dynamic of the system changes depending on the k value associated to the body force in the original SFM.

Fig. 2 shows the evacuation time as a function of the pedestrian's desired velocity. The evacuation time was defined as the time until 70% of the pedestrians left the room. The different markers correspond to different k values (*i.e.* different body "stiffness"). The crosses correspond to the Helbing original SFM parameter, the up-triangles correspond to the value measured in Ref ..., squares correspond to an absent body force and circles correspond to an extreme value of stiffness (one order of magnitude higher than the original SFM). The down triangles correspond to an intermediate value between the empirical value presented in Ref... and the chosen by Helbing in Ref...

There is a noticeable difference in the evacuation time depending on the k value of the body force. The higher the k the smaller the evacuation time, meaning that if pedestrians are stiffer, the overall speed increases (hence the evacuation time decreases).

The Faster-is-Faster (FIF) is the phenomenon in which under certain conditions, increasing the desired velocity yields to a reduction of the evacuation time. The Faster-is-Faster is the opposite effect (the higher v_d the lower the evacuation time). Notice that the presence of the Faster-is-Faster (FIF) effect and the Faster-is-Slower are dependent on the value of k. In Fig. 2 we can see that $k = 1.2$ E5 only exhibits FIS effect for v_d >2 m/s. When $k = 1.2$ E6, the evacuation time reduces as v_d increases, meaning that only FIF is reported. The explored values of k that satisfy $k \leq 6$ E4 exhibit both the FIS and the FIF effect depending on the range of desired velocities. Notice that the behavior of the case in which $k = 0$ is very similar to the case in which $k = 1.2$ E4.

Network analysis is a set of techniques that characterize the structures in a graph. We defined the graph of contacts among individuals. In this graph, each node represents a pedestrian and the link between a pair of nodes is

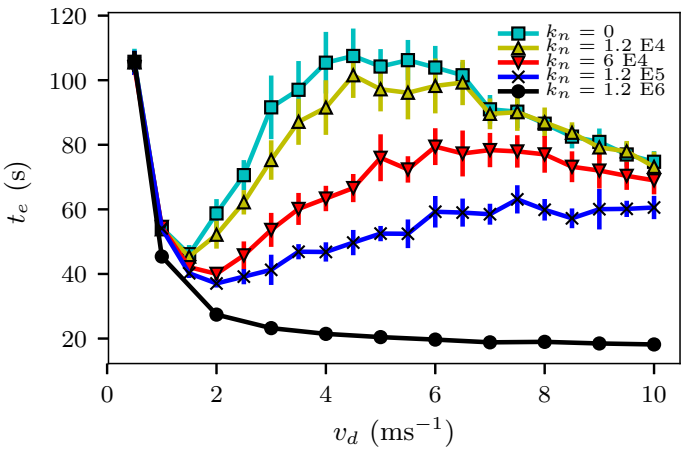

Figure 2: Mean evacuation time (s) vs. the pedestrians desired velocity (m/s) for a bottleneck. The room was 20 m x 20 m size. The door was 0.92 m width. Mean values were computed from 10 evacuation processes. 225 pedestrians were initially placed in a square lattice with a random initial velocity. Each process was finished when 158 pedestrians left the room. The different symbols indicate the k value corresponding to the body force (see the label).

settled if the pedestrians are in physical contact (*i.e.* $r_{ij} < Rij$).

Fig. 3a shows the mean degree of the contact graph as a function of the desired velocity. The degree of a node is defined as the amount of edges assigned to the node. This means, the number of pedestrians that are in physical contact with a given pedestrian. The mean degree is the average of the degree over all the nodes (pedestrians) and over the whole sampled time (from the time the system reaches the stationary state to the end of the simulation).

Increasing v_d increases the mean degree in all the cases. This happens because increasing v_d produces higher densities that force individuals to touch each other. For a given v_d the mean degree reduces as the k value increases. In other words, the stiffer the pedestrians the less they touch each other. We will later discuss that this phenomenon is restricted to the bottleneck geometry that cannot be extrapolated to the corridor geometry.

Fig. 3b shows the overlap as a function of v_d. The overlap is defined as

$R_{ij} - r_{ij}$ where R_{ij} is the sum of radius of particle i and particle j and r_{ij} is the distance between both particles. In the range $v_d \geq 2$ m/s we can see that increasing v_d increases the overlap (for all the k values studied). For a given v_d, the overlap increases as the k value decreases. Reducing k means reducing the normal body force which allows a greater invasion of the personal space of the individuals.

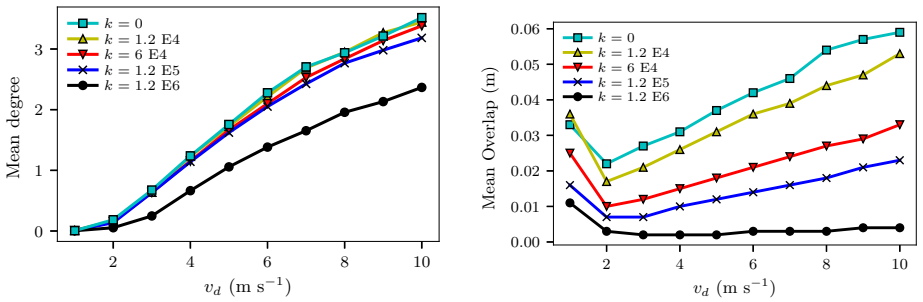

(a) (b)

Figure 3: (a) Mean degree as a function of the pedestrians desired velocity (m/s). (b) Mean overlap as a function of the pedestrians desired velocity (m/s). Each symbol indicates the k value corresponding to the body force (see the labels). The data corresponds to a bottleneck with periodic boundary conditions (re-injecting pedestrians). The average was taken every two seconds once the crowd reaches the stationary state (t =20 s) until the end of the simulation (t =110 s).

Increasing the stiffness has a significative impact on the evacuation dynamics. It reduces the overlap and reduces the mean degree between pedestrians. Both effects tend to reduce the friction in the crowd and the immediate consequence of this is a reduction of the evacuation time (pedestrians escape faster). The body force has a notorious impact in the number of pedestrians that each pedestrians touch (degree). This is clearly depicted in Fig. 4 where four different configurations of the evacuation dynamics are shown. The configurations represent 225 pedestrians trying to escape through a 0.92 m door which center is located at $(x, y) = (20, 10)$ m. The colors correspond to the degree of each node (pedestrian) and the lines between pedestrians represent the contacts among them.

The four configurations corresponds to two different v_d and two different k values. Fig. 4a represents v_d =2 and $k = 0$, Fig. 4b corresponds to v_d =10

and $k = 0$ while 4c and 4d correspond to v_d =2 and v_d =10 respectively and both have the same body force coefficient k =1.2 E6. As expected, increasing the desired velocity compress the crowd towards the exit.

Comparing Fig. 4a against Fig. 4c and Fig 4b against Fig. 4d it is clear that increasing the stiffness reduces the degree. The most notorious case is the pictures corresponding to v_d =10 in which, despite having the same v_d, the size of the bulk increases when the pedestrians are stiffer. Moreover, when pedestrians are stiffer they have fewer contacts in general (less degree). Notice that there are no pedestrians with degree 6 when k = 1.2 E6 and there are a lot of pedestrians with degree 6 when k=0.

4.2. Corridor

In this section, we present the results corresponding to the corridor geometry. We show how the overall dynamic of the system changes depending on the k value associated to the body force in the original SFM.

In Fig. 5 we show the flow as a function of the global density (fundamental diagram). 5a corresponds to non body force (*i.e.* $k_n = 0$), corresponds to a body force with k_n=1.2 E5. Each curve correspond to a different friction value. The circles correspond to the value of the original SFM ($\kappa = 2.4$ E5), the "+" symbol correspond to the original value increased by a factor of five and triangles correspond to the original value increased by a factor of ten.

According to most of the empirical measurements, the flow decreases for high enough values of density because the motion becomes jammed. Notice that the original friction does not produce a reduction of the flow when there is no body force but when the body force is included (with the original value), the flow reduces from 5 p m^{-2} to 7 p m^{-2} and increases for higher values of density. When the density is five times the original value, the flow reduces for densities higher than 5 p m^{-2} in both cases (with body force and without body force). The main qualitative difference is that including the body force produces a subtle increment in the flow for densities higher than 7 p m^{-2}. When the friction is increased by a factor of ten, the flow reduces or remains constant when the density is higher than 5 p m^{-2} for both cases (with body force and without body force). This result suggests that even including the body force, the original SFM requires an increment of the friction

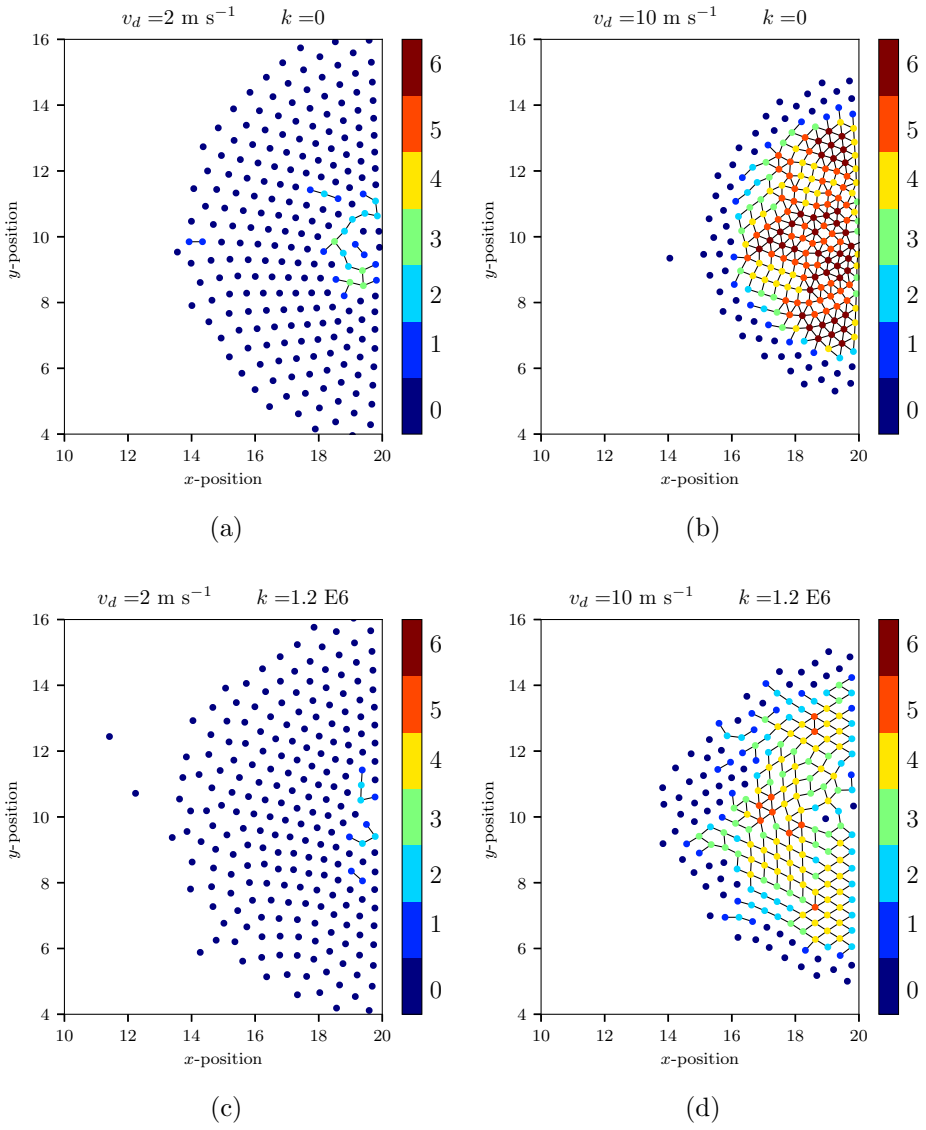

Figure 4: Contact networks of a 225 pedestrian evacuation through a bottleneck. The door is placed at $(x, y) = (20, 10)$ m, the width of the door is 0.92 m (equivalent to 2 pedestrian's diameter). The lines that connect the nodes (pedestrians) represent the contact between them. The color represents the degree (the number of pedestrians with which it is connected). 4a and 4b correspond to a simulation without body force with v_d =2 and v_d =10 respectively. 4c and 4d correspond to simulations with k=1.2 E6 with v_d =2 and v_d =10 respectively.

in order to reproduce the flow reduction reported in empirical measurements.

It is worth mentioning that increasing the body force reduces the flow, for a given density and a given friction value (compare 5a with 5b). In other words, pedestrians walk slower along the corridor if the k value increases (*i.e.* if they are stiffer). This result is the opposite of what we get in bottleneck geometry since the stiffer the pedestrians the faster they walk.

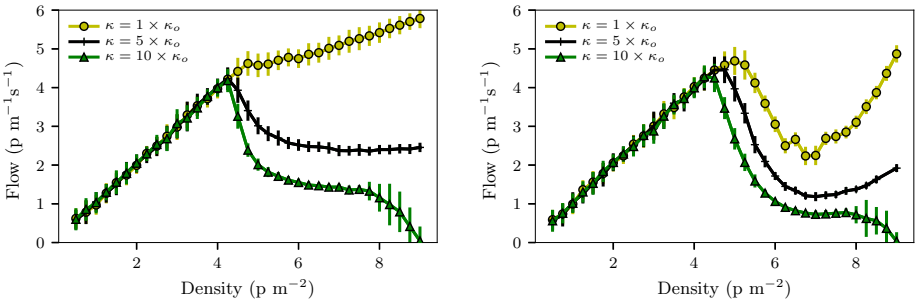

(a) (b)

Figure 5: Flow vs. global density. The flow is calculated in a circular area of R=1 m at the center of the corridor. The circle corresponds to the original friction of the SFM, the "+" symbol corresponds to the friction increased by a factor of five and the triangles correspond to the friction increased by a factor of ten. The desired velocity was $v_d = 1$ in all the cases. Fig. 5a corresponds to simulations without body force and Fig. 5b corresponds to a body force with k =1.2 E5.

To understand why in corridor geometry pedestrians walk slower as they become stiffer it is important to take into account that pedestrians walk slower if the friction increases. In corridors, the friction increases when pedestrians become stiffer because the crowd tends to cluster more. The clusterization means that more pedestrians are touching each other.

One way to analyze the clusterization is by creating a network out of the (x,y) positions of the pedestrians. In this network, each node represents a pedestrian and there is a link between a pair of nodes i, j if the pair of pedestrians represented by the nodes are touching each other (*i.e.* $r_{ij} \leq R_{ij}$). Once the network is created, it is possible to use the analytical tools that allow describing the configuration such as the mean degree, the distribution of clusters, the shortest path length, etc.

In Fig 6a we show the mean degree as a function of the global density for different k values. When the density is low, the degree is zero because the pedestrians do not touch each other. When the density is around 4.5, a few pedestrians start to touch each other increasing the mean degree. As the density increases, the mean degree increases too until reaching an asymptotic behavior in degree six. When the degree is six, it corresponds to the densest packing possible for identical hard circles, the result is a hexagonal packing arrangement.

It is important to notice that in Fig. 6a for a given value of density, the stiffer the pedestrians, the higher the degree. A higher degree means more friction force which is the cause of the reduction of the flow. In the bottleneck geometry, the opposite thing happens, the stiffer the pedestrians the lower the mean degree. This is the reason why in bottleneck pedestrians evacuate faster as they become stiffer while in corridor pedestrian's flow is lower as they become stiffer.

The mean overlap increases as the global density increases (see Fig. 6) and the higher the stiffness the lower the overlap. This result is similar to the overlap vs. the desired velocity obtained for bottleneck geometry. The higher the value of k the higher the repulsion of pedestrian-pedestrian interaction since the body force is acting in the normal direction n_{ij}.

As was mentioned above, increasing the k value of the body force increases the stiffness of pedestrians. Increasing the stiffness reduces the overlap (both in bottleneck and corridor) and reduces the mean degree in a bottleneck but increases the mean degree in a corridor. In Fig.7 it shown the network associated with the corridor at a particular timestep and a particular global density. Fig. 7a corresponds to $k = 0$ while Fig. 7 corresponds to $k = 1.2$ E5. This is an example to show how increasing the stiffness increases the number of contacts between pedestrians. Notice that there are many more pedestrians with degree 6 in the case of $k = 1.2$ E5 than the case of $k = 0$.

The increment of the clusterization is responsible for the reduction of the flow. In the corridor geometry, the crowd gets more clusterized if the pedestrians become stiffer. We studied the network properties of the contact graph arising from the positions (x, y) of every the pedestrians. We found that a

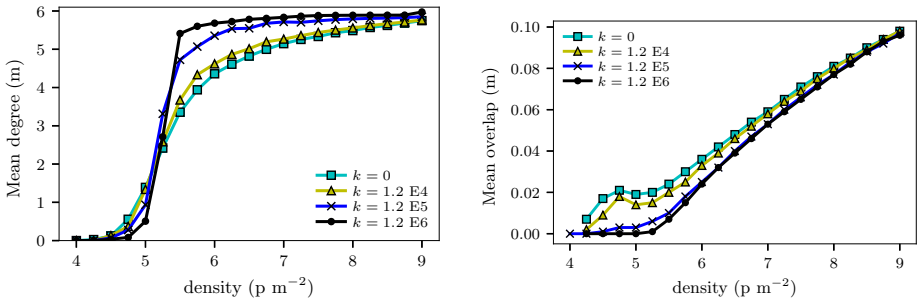

(a) (b)

Figure 6: 6a mean degree as a function of the global density for different k values. mean overlap as a function of the global density. The mean values are averages over all the pedestrians and over time once the system reaches the stationary state. Both measurements correspond to corridor geometry with desired velocity $v_d = 1$.

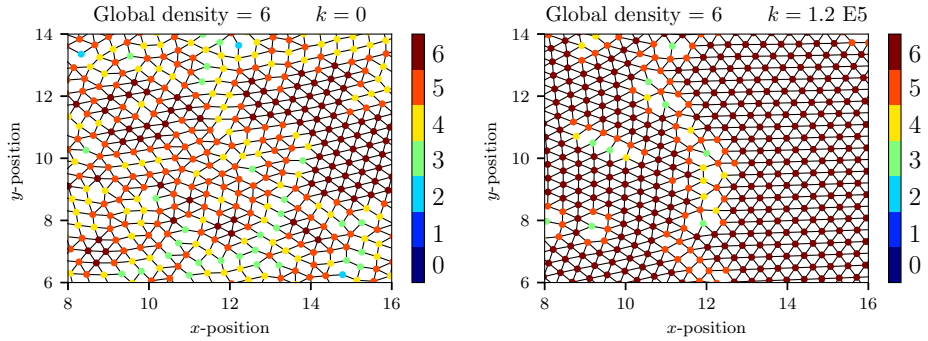

(a) (b)

Figure 7: Contact network of the pedestrians along the corridor. The lines that connect the nodes (pedestrians) represent the contact between them. The colors stand for the degree of the node (the number of pedestrians that are in contact with him/her). The corridor was 28 m $\times$ 22 m with periodic boundary conditions and $v_d = 1$. 7a corresponds to a simulation without body force and corresponds to a simulation with $k = 1.2$ E5.

good descriptor to exhibit the clusterization is the number of triangles per node. A triangle is defined as a structure composed of three nodes all in contact with each other. In Fig. 8 we show the triangles per node as a function of the global density for different stiffness values k. This descriptor allows to distinguish states with the same global density but different stiffness levels. In other words, it is a descriptor very sensitive to changes in stiffness that allow expressing the degree of clustering of the system even better than the mean degree.

This result is consistent with the results obtained in Ref. [36] where they explore several topological and geometric descriptors capable of properly describing granular systems with different stiffness. While our study system is self-propelled, there are analogies with the system studied in Ref. Like the authors, we recommend using topological descriptors (in particular triangles per node) to describe systems with equal global density and different stiffness levels.

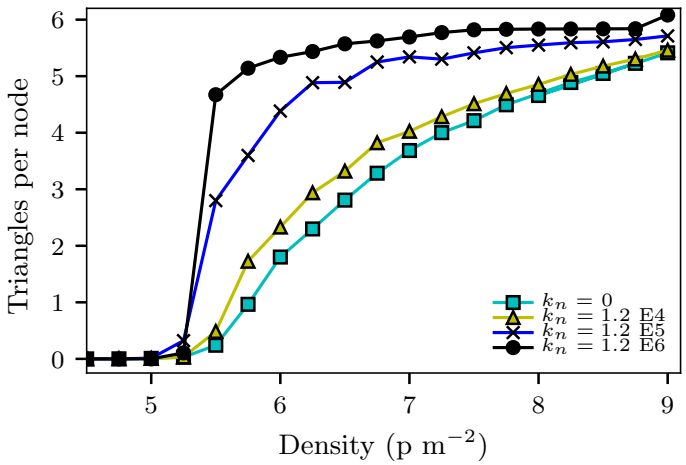

Figure 8: Triangles per node as a function of the global density. A triangle in a network is defined as three nodes all connected. Each marker corresponds to a different stiffness k (see the label in the plot). The measurements correspond to a corridor of 28 m $\times$ 22 m with periodic boundary conditions and $v_d = 1$.

4.3. Reduced-in-units equation of motion

5. Discussion

6. Conclusions

Acknowledgments

This work was supported by the National Scientific and Technical Research Council (spanish: Consejo Nacional de Investigaciones Científicas y Técnicas - CONICET, Argentina) grant Programación Científica 2018 (UBACYT) Number 20020170100628BA.

Appendix A. Reduced-in-units equation of motion

The SFM description in Section 3.1 introduces seven parameters (m, τ, v_d, B, A, κ and k) attaining for the "individual" behavior of each pedestrian. The collective dynamic, however, requires a smaller set of parameters. In order to identify this smaller set, we introduce the following unit-less magnitudes

$$\left\{ \begin{array}{rcl} t' & = & t/\tau \\ r' & = & r/B \\ v' & = & v/v_d \end{array} \right. \tag{A.1}$$

The equation of motion (1) can be written in terms of these (unit-less) magnitudes, while only three (reduced) parameters are needed.

$$\frac{d\mathbf{v}'}{dt'} = \hat{\mathbf{e}}_d - \mathbf{v}' + \mathcal{A}\, e^{R'-r'}\, \hat{\mathbf{n}} + g(R'-r') \left[\mathcal{K}\, (\Delta\mathbf{v}' \cdot \hat{\mathbf{t}})\, \hat{\mathbf{t}} + \mathcal{K}_c\, \hat{\mathbf{n}} \right] \tag{A.2}$$

where the smaller set ($\mathcal{A}$,$\mathcal{K}$,$\mathcal{K}_c$) means

$$\mathcal{A} = \frac{A\,\tau}{m\,v_d} \quad , \quad \mathcal{K} = \frac{\kappa\,B\,\tau}{m} \quad , \quad \mathcal{K}_c = \frac{k\,B\,\tau}{m\,v_d} \tag{A.3}$$

Notice that the SFM will arrive to similar collective dynamics whenever the reduced set ($\mathcal{A}$,$\mathcal{K}$,$\mathcal{K}_c$) remains unchanged (although some "individual"

parameters are allowed to change). For a deep explanation on the meaning of the set ($\mathcal{A}$,$\mathcal{K}$,$\mathcal{K}_c$) see Section 3.2.

[1] D. Helbing, I. Farkas, and T. Vicsek. Simulating dynamical features of escape panic. *Nature*, 407:487–490, 2000.

[2] D. Parisi and C. Dorso. Microscopic dynamics of pedestrian evacuation. *Physica A*, 354:606–618, 2005.

[3] D. Parisi and C. Dorso. Morphological and dynamical aspects of the room evacuation process. *Physica A*, 385:343–355, 2007.

[4] G. Frank and C. Dorso. Room evacuation in the presence of an obstacle. *Physica A*, 390:2135–2145, 2011.

[5] Colin M. Henein and Tony White. Macroscopic effects of microscopic forces between agents in crowd models. *Physica A: Statistical Mechanics and its Applications*, 373:694 – 712, 2007.

[6] J. Fruin. The causes and prevention of crowd disasters. In R.A. Smith and J.F. Dickie, editors, *Engineering for Crowd Safety*. Elsevier, 1993.

[7] Taras I. Lakoba, D. J. Kaup, and Neal M. Finkelstein. Modifications of the helbing-molnr-farkas-vicsek social force model for pedestrian evolution. *SIMULATION*, 81(5):339–352, 2005.

[8] Paul A. Langston, Robert Masling, and Basel N. Asmar. Crowd dynamics discrete element multi-circle model. *Safety Science*, 44(5):395 – 417, 2006.

[9] Peng Lin, Jian Ma, You-Ling Si, Fan-Yu Wu, Guo-Yuan Wang, and Jian-Yu Wang. A numerical study of contact force in competitive evacuation. *Chinese Physics B*, 26(10):104501, sep 2017.

[10] I. M. Sticco, F. E. Cornes, G. A. Frank, and C. O. Dorso. Beyond the faster-is-slower effect. *Phys. Rev. E*, 96:052303, Nov 2017.

[11] Rahul Narain, Abhinav Golas, Sean Curtis, and Ming C. Lin. Aggregate dynamics for dense crowd simulation. *ACM Trans. Graph.*, 28(5):122:1–122:8, December 2009.

[12] N. Pelechano, J.Allbeck, and N. Badler. Controlling individual agents in high-density crowd simulation. *Proceedings of the 2007 ACM SIGGRAPH/Eurographics Symposium on Computer Animation*, pages 99–108, 2007.

[13] Mehdi Moussaïd, Dirk Helbing, and Guy Theraulaz. How simple rules determine pedestrian behavior and crowd disasters. *Proceedings of the National Academy of Sciences*, 108(17):6884–6888, 2011.

[14] Fernando Alonso-Marroquín, Jonathan Busch, Coraline Chiew, Celia Lozano, and Álvaro Ramírez-Gómez. Simulation of counterflow pedestrian dynamics using spheropolygons. *Phys. Rev. E*, 90:063305, Dec 2014.

[15] Arianna Bottinelli and Jesse L. Silverberg. How to: Using mode analysis to quantify, analyze, and interpret the mechanisms of high-density collective motion. *Frontiers in Applied Mathematics and Statistics*, 3:26, 2017.

[16] J. Song, F. Chen, Y. Zhu, N. Zhang, W. Liu, and K. Du. Experiment calibrated simulation modeling of crowding forces in high density crowd. *IEEE Access*, 7:100162–100173, 2019.

[17] Bachar Kabalan. *Crowd dynamics : modeling pedestrian movement and associated generated forces*. Theses, Université Paris-Est, January 2016.

[18] A. Jebrane, P. Argoul, A. Hakim, and M. El Rhabi. Estimating contact forces and pressure in a dense crowd: Microscopic and macroscopic models. *Applied Mathematical Modelling*, 74:409 – 421, 2019.

[19] Litao Wang and Shifei Shen. A pedestrian dynamics model based on heuristics considering contact force information and static friction. *Transportmetrica B: Transport Dynamics*, 7(1):1117–1129, 2019.

[20] I.M. Sticco, G.A. Frank, F.E. Cornes, and C.O. Dorso. A re-examination of the role of friction in the original social force model. *Safety Science*, 121:42 – 53, 2020.

[21] Yaouen Fily, Silke Henkes, and M. Cristina Marchetti. Freezing and phase separation of self-propelled disks. *Soft Matter*, 10:2132–2140, 2014.

[22] Milad Haghani, Majid Sarvi, and Zahra Shahhoseini. When push does not come to shove: Revisiting faster is slower in collective egress of human crowds. *Transportation Research Part A: Policy and Practice*, 122:51 – 69, 2019.

[23] Dirk Helbing, Anders Johansson, and Habib Zein Al-Abideen. Dynamics of crowd disasters: An empirical study. *Phys. Rev. E*, 75:046109, Apr 2007.

[24] Rainald Lohner, Britto Muhamad, Prabhu Dambalmath, and Eberhard Haug. Fundamental diagrams for specific very high density crowds. *Collective Dynamics*, 2, 2018.

[25] Dirk Helbing and Péter Molnár. Social force model for pedestrian dynamics. *Phys. Rev. E*, 51:4282–4286, May 1995.

[26] Anders Johansson. Constant-net-time headway as a key mechanism behind pedestrian flow dynamics. *Phys. Rev. E*, 80:026120, Aug 2009.

[27] Meifang Li, Yongxiang Zhao, Lerong He, Wenxiao Chen, and Xianfeng Xu. The parameter calibration and optimization of social force model for the real-life 2013 yaan earthquake evacuation in china. *Safety Science*, 79:243 – 253, 2015.

[28] Ulrich Weidmann. Transporttechnik der fussgänger. *IVT Schriftenreihe*, 90, Jan 1992.

[29] S.P. Hoogendoorn and W. Daamen. Microscopic Calibration and Validation of Pedestrian Models: Cross-Comparison of Models Using Experimental Data. In A. Schadschneider, T. Pöschel, R. Kühne, M. Schreckenberg, and D. E. Wolf, editors, *Traffic and granular flow '05*, volume Part III. Springer, 2007.

[30] A. Seyfried, B. Steffen, W. Klingsch, Th. Lippert, and M. Boltes. The Fundamental Diagram of Pedestrian Movement Revisited - Empirical Results and Modelling. In A. Schadschneider, T. Pöschel, R. Kühne, M. Schreckenberg, and D. E. Wolf, editors, *Traffic and granular flow '05*, volume Part III. Springer, 2007.

[31] A. Johansson, D. Helbing, and P.K. Shukla. Specification of the social force pedestrian model by evolutionary adjustment to video tracking data. *Advances in Complex Systems*, 10(supp02):271–288, 2007.

[32] Mehdi Moussaï d, Dirk Helbing, Simon Garnier, Anders Johansson, Maud Combe, and Guy Theraulaz. Experimental study of the behavioural mechanisms underlying self-organization in human crowds. *Proceedings of the Royal Society B: Biological Sciences*, 276(1668):2755–2762, 2009.

[33] M. Luber, J. A. Stork, G. D. Tipaldi, and K. O. Arras. People tracking with human motion predictions from social forces. In *2010 IEEE International Conference on Robotics and Automation*, pages 464–469, May 2010.

[34] Stefan Seer, Christian Rudloff, Thomas Matyus, and Norbert Brändle. Validating social force based models with comprehensive real world motion data. *Transportation Research Procedia*, 2:724 – 732, 2014. The Conference on Pedestrian and Evacuation Dynamics 2014 (PED 2014), 22-24 October 2014, Delft, The Netherlands.

[35] S. M. P. Siddharth and P. Vedagiri. Modeling the gender effects of pedestrians and calibration of the modified social force model. *Transportation Research Record*, 2672(31):1–9, 2018.

[36] Arévalo, Roberto and Pugnaloni, Luis A and Zuriguel, Iker and Maza, Diego Contact network topology in tapped granular media. *Physical Review E*, 87(2):022203, 2013.